Eur. Phys. J. B **36**, 313–316 (2003)
DOI: 10.1140/epjb/e2003-00349-2

THE EUROPEAN PHYSICAL JOURNAL B

Field-domain dynamics in negative-effective-mass terahertz oscillators

J.C. Cao[1,a] and H.C. Liu[2]

[1] State Key Laboratory of Functional Materials for Informatics, Shanghai Institute of Microsystem and Information Technology, Chinese Academy of Sciences, 865 Changning Road, Shanghai 200050, P.R. China
[2] Institute for Microstructural Sciences, National Research Council, Ottawa, Ontario K1A 0R6, Canada

Received 18 July 2003
Published online 23 December 2003 – © EDP Sciences, Società Italiana di Fisica, Springer-Verlag 2003

Abstract. We have theoretically studied electric-field-domain dynamics and current self-oscillations in dc-biased negative-effective-mass (NEM) p^+pp^+ diodes. The formation and traveling of electric-field domains in the diodes are investigated in detail with a realistic treatment of the scatterings contributions from carrier-impurity, carrier-acoustic phonon, and carrier-optic phonon within the balance-equation theory. The interesting patterns of the spatiotemporal electric-field domains are shown as a gray density plot with the applied bias as a controlling parameter. It is found that, the applied bias could largely influence the current patterns and self-oscillating frequencies, which lie in the THz range for the NEM p^+pp^+ diode with a submicrometer p-base. The NEM p^+pp^+ diode may therefore be developed as an electrically tunable THz-frequency oscillator.

PACS. 73.61.Ey III-V semiconductors – 73.50.Fq High-field and nonlinear effects – 85.30.Fg Bulk semiconductor and conductivity oscillation devices (including Hall effect devices, space-charge-limited devices, and Gunn effect devices) – 85.30.De Semiconductor-device characterization, design, and modeling

1 Introduction

Much effort has recently been devoted to experimental and theoretical studies of the terahertz (THz) oscillators [1–3], owning to its promising applications in stratospheric astronomy, medical imaging, and large capacity mobile communication. Different electronic approaches to realize THz radiations are reported, such as Gunn devices [4], superlattice oscillators [5,6], and negative-effective-mass oscillators (NEM) [7,8]. Experiments [9,10] show that the dispersion relation for the ground subband of a p-type quantum well (QW) of zink-blende-like semiconductors contains an extensive section with NEM due to the spin-orbit coupling of heavy- and light-hole states and the symmetry breaking of the quantum well potential. By assuming an analytical NEM dispersion relation, the model calculations of carrier transport in p^+pp^+ diodes with a NEM p-base have been performed, by using the collisionless Boltzmann equation [11–13] and the nonparabolic balance equation theory [7,8,14]. Calculations [7] indicated that the steady-state velocity-field curve of carriers with a NEM dispersion contains a N-shaped negative-differential-velocity (NDV) region, which can lead to the formation of electric-field domains and self-oscillating currents in the dc-biased NEM p^+pp^+ diode. The oscillating features mainly depend on the form of the dispersion relation, thus the self-oscillating frequency may be controlled by changing the dispersion relation. The self-oscillating frequency lies in the THz range for the submicrometer NEM p^+pp^+ diode.

The purpose of the paper is to study field-domain dynamics and self-oscillating current patterns in the NEM p^+pp^+ diodes with the applied bias as a controlling parameter. In the calculations, we have accurately included different scattering contributions by impurity, acoustic phonon, and optic phonon within the balance-equation theory. The resulting N-shaped velocity-field relation is then fed into the transient drift-diffusion model and Poisson equation to study spatiotemporal electric-field domain and self-oscillating characteristics of the NEM p^+pp^+ diode. Detail calculations indicate that the carriers having a NEM may give rise to a rich variety of spatiotemporal current patterns and self-oscillating behaviors. Both the applied bias and the doping concentration could influence the patterns and self-oscillating frequencies.

2 Negative differential velocity of negative-effective-mass semiconductors

We consider a model NEM dispersion expressed by [7,11],

$$\varepsilon(\mathbf{k}) = \frac{1}{2}\left[\frac{\hbar^2\mathbf{k}^2}{2m_e} - \sqrt{\left(\frac{\hbar^2\mathbf{k}^2}{2M_e} - \varepsilon_0\right)^2 + 4\Delta^2} + \sqrt{\varepsilon_0^2 + 4\Delta^2}\right], \tag{1}$$

in which $\mathbf{k} = (k_x, k_y, k_z)$ is the three-dimensional wave-vector, $m_e \equiv Mm/(M+m)$, and $M_e \equiv Mm/(M-m)$

[a] e-mail: jccao@mail.sim.ac.cn

with m and M two effective masses, Δ and ε_0 are two energy-band-related energies, and $C \equiv \sqrt{\varepsilon_0^2 + 4\Delta^2} - \varepsilon_0$, When $M \to m$, the dispersion (1) reduces to a parabolic band $\varepsilon(\mathbf{k}) = \hbar^2\mathbf{k}^2/(2m)$. In the calculations, we set $\varepsilon_0 = 0.1$ eV, $\Delta = 0.02$ eV, $m = 0.085m_0$ (m_0 is the free electron mass), and $M = 0.44m_0$, respectively. According to the nonparabolic balance-equation theory [7,8,14], when a uniform electric field $\mathbf{E}$ is applied to the semiconductor with the dispersion $\varepsilon(\mathbf{k})$, the transport state of the carriers can be described by the average center-of-mass momentum $\mathbf{p}_d$ and the relative carrier temperature T_c, which are determined by the effective acceleration and energy-balance equations [7,8,14],

$$0 = en\mathbf{E}\cdot\mathcal{K} + \mathbf{A}_{\rm ei} + \mathbf{A}_{\rm ep}, \tag{2}$$

$$0 = en\mathbf{E}\cdot\mathbf{v}_d - W_{\rm ep}, \tag{3}$$

in which e is the carrier charge, and

$$n = \frac{1}{4\pi^3}\int d^3k f\left(\left(\varepsilon\left(\mathbf{k}\right) - \mu\right)/k_{\rm B}T_c\right) \tag{4}$$

is the carrier density, $\mathbf{v}_d = \langle\nabla\varepsilon\left(\mathbf{k}\right)\rangle$ is the average velocity, $\varepsilon = \langle\varepsilon\left(\mathbf{k}\right)\rangle$ is the average energy, and $\mathcal{K} = \langle\nabla\nabla\varepsilon\left(\mathbf{k}\right)\rangle$ is the ensemble-averaged inverse-effective-mass tensor of the carriers. Here $\langle\cdots\rangle$ stands for the weighted integral over a Brillouin zone in $\mathbf{k}$-space: $\langle\cdots\rangle = 1/(4\pi^3 n)\int d^3k f\left(\left[\varepsilon\left(\mathbf{k}-\mathbf{p}_d\right)-\mu\right]/k_{\rm B}T_c\right)\cdot\cdot\cdot$, with $f(x) = 1/\left[\exp\left(x\right)+1\right]$ the Fermi distribution function and μ the chemical potential. The frictional acceleration $\mathbf{A}_{\rm ei}$, $\mathbf{A}_{\rm ep}$ (due to impurity and phonon scatterings) and the energy-loss rate $W_{\rm ep}$ (due to phonon scattering), share the same expressions as those given in reference [14]. They are completely determined by $\mathbf{p}_d$, T_c, and μ (or n) for a semiconductor system with known impurity distributions, phonon modes, electron-impurity potentials, and electron-phonon coupling matrix elements. The explicit expressions of the acceleration and energy-loss rate can be found in reference [7].

We have calculated the carrier drift velocity v_d as a function of the steady-state electric field E at the lattice temperature $T = 77$ K, by accounting for the scatterings from carrier-impurity, carrier-acoustic-phonon (deformation and piezoelectric), and carrier-optic-phonon. All material constants used in calculations are typical values of GaAs: lattice density $d = 5.31$ g/cm3, transverse sound velocity $v_{st} = 2.48\times10^3$ m/s, longitudinal sound velocity $v_{sl} = 5.29\times10^3$ m/s, LO phonon energy $\Omega_{\rm LO} = 35.4$ meV, low-frequency dielectric constant $\kappa = 12.9$, optical dielectric constant $\kappa_\infty = 10.8$, valence-band deformation potential $\Xi = 8.5$ eV, and piezoelectric constant $e_{14} = 1.41\times10^9$ V/m. In Figure 1 we show the velocity-field relation of the NEM semiconductor at $T = 77$ K. Solid circles and squares are calculated from the balance equations (2, 3) respectively for the parabolic band and for the NEM dispersion. The solid line is the analytic fit by the expression

$$v_d = C_1E\left[1 - C_2\frac{E^2+C_3}{E^2+C_4E+C_5} + C_6\arctan(C_7E - C_8)\right], \tag{5}$$

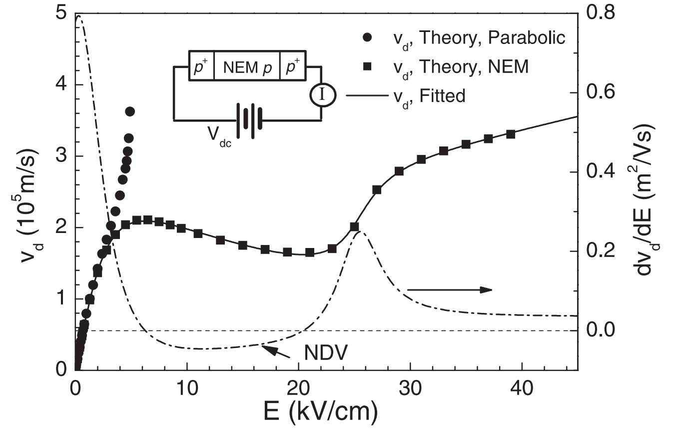

Fig. 1. Velocity-field relation (left axis) of the NEM semiconductor at lattice temperature $T = 77$ K. The solid circles are calculated from the balance equations for the parabolic band, the solid squares are calculated from the balance equations for the NEM dispersion, and solid line is the analytic fit by equation (5). The right axis shows the corresponding differential velocity by equation (6). There is a region of electric field where the differential velocity is negative. The inset shows the dc-biased p^+pp^+ NEM diode structure studied here.

in which the values of the parameters are $C_1 = 1.36204$, $C_2 = 1$, $C_3 = 5.46062$, $C_4 = 1.34883$, $C_5 = 13.57118$, $C_6 = 0.01738$, $C_7 = 0.42774$, and $C_8 = 10.82297$ at lattice temperature $T = 77$ K. The right axis of Figure 1 shows the corresponding differential velocity of equation (5), i.e.,

$$\frac{{\rm d}v_d}{{\rm d}E} = C_1\left[1 - C_2\frac{E^2+C_3}{E^2+C_4E+C_5} + C_6\arctan(C_7E-C_8)\right] + C_1E\left[\frac{-2C_2E}{E^2+C_4E+C_5} + \frac{C_2(E^2+C_3)(2E+C_4)}{(E^2+C_4E+C_5)^2} + \frac{C_6C_7}{1+(C_7E-C_8)^2}\right]. \tag{6}$$

The most important features of equation (6) is that, there is a region where differential velocity becomes negative. The inset of Figure 1 shows the dc-biased p^+pp^+ NEM diode structure studied here. The NEM-induced NDV is the origin of the formation of electric-field domain and current self-oscillation in the present NEM diodes.

3 Field-domain dynamics and current self-oscillation

The velocity-field relation expressed by equation (5) is fed into the transient drift-diffusion model and the Poisson equation to study the electric-field domain and current self-oscillation of the dc-biased NEM p^+pp^+ diode. We solve the spatial and temporal evolution of the electrostatic potential and carrier density as two fundamental variables, which are self-consistently used to calculate all other transport quantities. The total current density $J(t)$

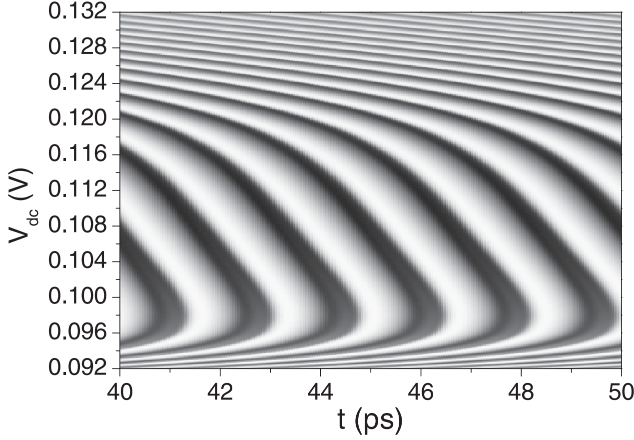

Fig. 2. Time-periodic self-oscillating current densities of the NEM p^+pp^+ diode at different dc biases are shown as a density gray plot, where lighter areas correspond to larger amplitudes of the current densities. The p-base length of the NEM p^+pp^+ diode is set to be 0.1 μm, and the p-base doping concentration is $N_a = 3 \times 10^{17}$ cm^{-3}. The lattice temperature is $T = 77$ K.

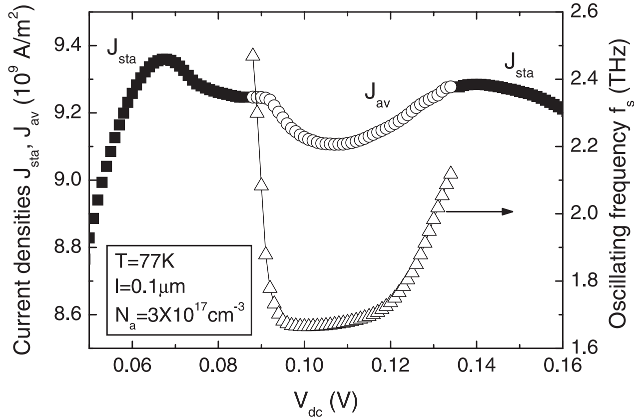

Fig. 3. Dependence of the time-averaged current density $J_{\rm av}$, static current density $J_{\rm sta}$, and self-oscillating frequency f_s (right axis) on the dc biases from 0.05 to 0.16 V.

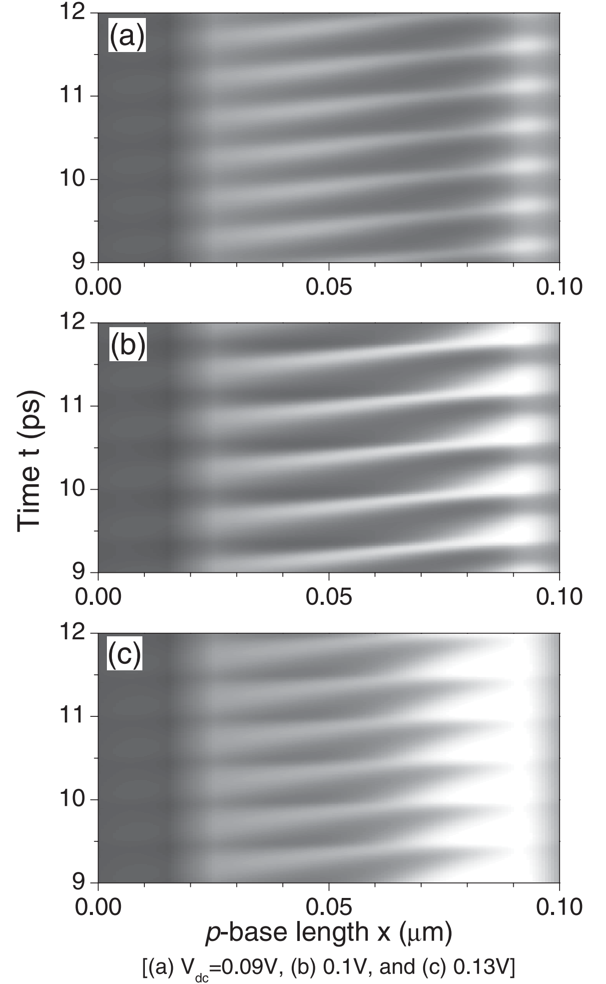

Fig. 4. Spatiotemporal electric-field domains are shown as a density gray plot, where lighter areas correspond to larger amplitudes of the electric fields. The applied dc biases are: (a) $V_{\rm dc} = 0.09$ V, (b) 0.1 V, and (c) 0.13 V, respectively. The parameters are same as those in Figure 2.

is the sum of the conduction current density and the displacement current density,

$$J(t) = env_d + \kappa\varepsilon_0 \frac{\partial E(x,t)}{\partial t}, \quad (7)$$

which is a function of time t only. When the diode is biased in the NDV region, a small doping inhomogeneity can cause the growth of a carrier accumulation layer and lead to the formation of high-field domain and current self-oscillation. Throughout the paper, the p-base length of the NEM p^+pp^+ diodes is set to be $l = 0.1$ μm, the doping concentration in the contact p^+-region is assumed to be $N_a^+ = 2 \times 10^{18}$ cm^{-3}, and the p-region doping concentration is $N_a = 3 \times 10^{17}$ cm^{-3}. The lattice temperature is set to be $T = 77$ K. When a dc bias, $V_{\rm dc}$, is applied to the NEM p^+pp^+ diode, it's found that there is a region of dc voltage band, $V_{\rm dc} \in$[0.088, 0.134 V], in which the dynamic electric-field domain is developed and the self-oscillating current shows up with a frequency f_s. When the dc voltage is beyond the dynamic dc voltage band, only the static electric-field domain is formed, i.e., the current density approaches a constant (defined as $J_{\rm sta}$) after the initial transient dies out. Time-periodic self-oscillating current densities at different dc biases $V_{\rm dc}$ are shown in Figure 2 as a density gray plot, where lighter areas correspond to larger amplitudes of the current densities. The oscillating patterns and their frequencies are obviously different when changing $V_{\rm dc}$. We define the time-averaged current density $J_{\rm av}$ by integrating $J(t)$ over one oscillating period ($= 1/f_s$). In Figure 3 we show the dependence of time-averaged current density $J_{\rm av}$, static current density $J_{\rm sta}$, and self-oscillating frequency f_s (right axis) on the dc bias from $V_{\rm dc} = 0.05$ to 0.16 V. The region of $V_{\rm dc} \in$[0.088, 0.134 V] shown by open circles is the dynamic band, in which the self-oscillating frequency is changed from about 1.68 THz to 2.49 THz. To have a clear insight into spatiotemporal evolution of carrier dynamics, In Figure 4 we have shown the spatiotemporal electric-field domains as a density gray plot at different biases: (a) $V_{\rm dc} = 0.09$ V,

(b) 0.1 V, and (c) 0.13 V, respectively, where lighter areas correspond to larger amplitudes of the electric fields. It's clearly seen that the electric-field domain periodically travels in the p-base with the evolution of time, and the electric field increases with increasing the dc bias.

4 Conclusions

The dependence of current self-oscillation and its patterns on the applied bias are investigated in the dc biased NEM p^+pp^+ diode. When the NEM p^+pp^+ diode is biased in the negative-differential-velocity region, the dynamic electric field domain is formed, leading to a current self-oscillation with a frequency in the THz range. The interesting patterns of spatiotemporal self-oscillating currents and field-domain dynamics are presented when changing the dc bias. The NEM-induced current self-oscillation may therefore be used to develop a tunable THz-frequency oscillator. We would mention that, in the present calculations the lattice temperature is set to be 77 K. When the NEM p^+pp^+ diode works at room temperature the present theory predicts a similar result, but the oscillating frequency somewhat decreases with increasing the lattice temperature.

This work was supported by the key National Natural Science Foundation of China, the Special Funds for Major State Basic Research Project (2001CCA02800G and 20000683), and the Special Funds for Shanghai Optic Engineering (011661075). The authors would like to thank Prof. X. L. Lei for many helpful discussions.

References

1. P.H. Siegel, IEEE Trans. Microwave Theory Tech. **50**, 910 (2002)
2. B. Ferguson, X.C. Zhang, Nature Materials **1**, 26 (2002)
3. H.C. Liu, C.Y. Song, Z.R. Wasilewski, A.J. SpringThorpe, J.C. Cao, C. Dharma-wardana, G.C. Aers, D.J. Lockwood, J.A. Gupta, Phys. Rev. Lett. **90**, 077402 (2003)
4. H. Eisele, A. Rydberg, G.I. Haddad, IEEE Trans. Microwave Theory Tech. **48**, 626 (2000)
5. E. Schomburg, N.V. Demarina, K.F. Renk, Phys. Rev. B **67**, 155302 (2003)
6. R. Scheuerer, M. Haeussler, K.F. Renk, E. Schomburg, Yu. Koschurinov, D.G. Pavel'ev, N. Maleev, V. Ustinov, A. Zhukov, Appl. Phys. Lett. **82**, 2826 (2003)
7. J.C. Cao, H.C. Liu, X.L. Lei, J. Appl. Phys. **87**, 2867 (2000)
8. J.C. Cao, X.L. Lei, Phys. Rev. B **67**, 085309 (2003)
9. R.K. Hayden, D.K. Maude, L. Eaves, E.C. Valadares, M. Henini, F.W. Shears, O.H. Hughes, J.C. Portal, L. Cury, Phys. Rev. Lett. **66**, 1749 (1991)
10. J.A. Kash, M. Zachau, M.A. Tischler, U. Ekenberg, Semicond. Sci. Technol. **9**, 681 (1994)
11. Z.S. Gribnikov, A.N. Korshak, N.Z. Vagidov, J. Appl. Phys. **80**, 5799 (1996)
12. A.N. Korshak, Z.S. Gribnikov, N.Z. Vagidov, V.V. Mitin, Appl. Phys. Lett. **75**, 2292 (1999)
13. R.R. Bashirov, Z.S. Gribnikov, N.Z. Vagidov, V.V. Mitin, Appl. Phys. Lett. **77**, 3785 (2000)
14. X.L. Lei, N.J.M. Horing, H.L. Cui, Phys. Rev. Lett. **66**, 3277 (1991)